THE RADIOLOGICAL RESEARCH ACCELERATOR FACILITY

An NIH-Supported Resource Center

WWW.RARAF.ORG

Director: David J. Brenner, Ph.D., D.Sc.
Associate Director: Gerhard Randers-Pehrson, Ph.D.
Manager: Stephen A. Marino, M.S.

Research Using RARAF

For almost two decades, many of the biology studies at RARAF, including those involving animals, have examined the "bystander" effect - the response of cells that are not directly irradiated but in close contact with, nearby, or only in the presence of irradiated cells. The emphasis of many of the present biological experiments is to determine the mechanism(s) by which the effect is transmitted, such as the direct gap junction communication through cell membrane contact and the pathways involved. Both the Microbeam and the Track Segment Facilities continue to be utilized in various investigations of this phenomenon. Research into bystander effects in 3-D systems continued this past year with the irradiations of *C. elegans* nematodes using a "worm clamp" system adapted for use on the microbeam system and microbeam irradiations of the ears of hairless mice.

The experiments performed using the RARAF Singletron between January 1 and December 31, 2012 and the number of shifts each was run in this period are listed in Table I. Fractional shifts are assigned when experimental time is shared among several users (*e.g.*, track segment experiments) or when experiments run for more or less than an 8-hour shift. Use of the accelerator

Table I. Experiments Run at RARAF January 1 - December 31, 2012

Exp No.	Experimenter	Institution	Exp. Type	Title of Experiment	Shifts Run
110	T. K. Hei	CRR	Biol.	Identification of molecular signals of alpha particle-induced bystander mutagenesis	62.3
113	A. Miller	AFRRI	Biol.	Role of alpha particle radiation in depleted uranium-induced cellular effects	1.6
144	O. Hobert	Columbia Univ.	Biol.	Microbeam irradiation of *C. elegans*	3.6
153	H. Lieberman	CRR	Biol.	The role of Rad9 in mediating global gene expression in directly irradiated and bystander cells	5.6
157	Brian Ponnaiya	CRR	Biol.	γH2AX production by low-energy X-rays	11.0
159	Lubomir Smilenov	CRR	Biol.	Bystander effect mechanisms	4.2
160	Doug Spitz	University of Iowa	Biol.	Cellular oxidation of radiation-induced free radicals	5.2
161	Jan Vijg	Albert Einstein College of Medicine	Biol.	Mutation spectrum of individual microbeam irradiated cells	3.2
163	Lubomir Smilenov	CRR	Biol.	Bystander effects in the hairless mouse ear	2.4
164	Lubomir Smilenov	CRR	Biol.	Mouse irradiation using IND spectrum neutrons	1.8
165	Helen Turner	CRR	Biol.	Blood irradiation using IND spectrum neutrons	1.6
166	Andre Nussenzweig	NCI	Biol.	Chromatin restructuring as a function of microbeam induced DNA DSBs	1.2
167	Eduoard Azzam	UMDNJ	Biol.	Radiation-induced DNA damage in bystander cells with inducible gap junction intercellular communication	0.8
168	Roger Howell	UMDNJ	Biol.	Bystander effects as a function of distance from irradiated cells in an *in vivo*-like system	0.2
169	Vincent LiCata	LSU	Biol.	The denatured states of a thermophilic versus a mesophilic DNA polymerase after charged particle irradiation	1.2

for experiments was 47% of the regularly scheduled time (40 hours per week), almost double what was used last year. Fifteen different experiments were run during this period. Seven experiments were undertaken by members of the CRR, including researchers at Columbia University who are not part of the CRR, supported by grants from the National Institutes of Health (NIH), the Department of Energy (DoE) and the National Institute of Allergies and Infectious Diseases (NIAID). Eight experiments were performed by external users, supported by grants and awards from the DoE, the Department of Defense (DoD), the NIH, the National Science Foundation (NSF), the Economic Community Cooperation Programme, the National Science Foundation of China, the National Cancer Institute (NCI), and a Louis V. Gestetner Jr. Scholar Award. Brief descriptions of these experiments follow.

Experiments to identify the signal transduction pathways involved in radiation-induced bystander responses (Exp. 110) were continued by Tom Hei of the CRR and several members of his group. Using the Microbeam Facility, they investigated mechanisms by which cytoplasmic stimuli modulate mitochondrial dynamics and functions in human small airway epithelial (SAE) cells. Cells were typically irradiated in the cytoplasm with ten ^{4}He ions. Control SAEC cells showed the usual elongated and tubular mitochondrial structure, whereas irradiated cells had a shortened and fragmented morphology. Moreover, cells irradiated in the cytoplasm demonstrated a reduction in cytochrome C-oxidase as well as succinate dehydrogenase activities when compared with non-irradiated controls, suggestive of reduced respiratory chain function. Irradiations were performed to determine if a bystander response exists in mouse embryonic stem cells (MESC) in ways similar to what has been reported previously for other cell lines. A lethal dose of 30 alpha particles was delivered through the nucleus in 10% of the cell population; the remaining (bystander) cells were examined for possible biological changes. COX-2 wild type (WT) and knockout (KO) mouse embryo fibroblasts (MEF) cells were irradiated with α-particles through the nucleus. The MEF cells were then fixed at different time points after irradiation and levels of γ-H2AX and 8-OHdG were quantified using immunochemical staining. Results indicated that both the number of γH2AX foci/cell and the expression level of 8-OHdG in non-irradiated bystander MEF cells peaked 60 minutes post-irradiation. When compared with control cells under similar conditions, the changes of γH2AX (~1.6 fold) and 8-OHdG (~2.6 fold) were significantly increased in COX-2 WT cells, but not significantly altered in the KO cells. Furthermore, relative to the control cells the micronucleus induction in bystander MEF cells 24 h post-irradiation increased significantly in the WT cells (~2.5 fold) but not in KO cells. Finally, the spi-mutant yield was significantly increased in bystander COX-2 WT MEF cells (~1.6 fold) relative to controls.

The exposure of military personnel and civilians to the alpha emitter and heavy metal depleted uranium (DU) is of concern to the Department of Defense. Studies using the Track Segment Facility to evaluate DU radiation-induced carcinogenesis and other late effects using *in vitro* models and to test safe and efficacious medical countermeasures (Exp. 113) were continued by Alexandra Miller of the Armed Forces Radiobiological Research Institute (AFFRI). Irradiations were performed to determine whether alpha particle radiation exposure of murine bone marrow stromal cells *in vitro* induces malignant transformation of un-irradiated co-cultivated hematopoietic stem cells, whether this is a chemical or radiation event, whether it involves cell-cell communication, and whether it involves reactive oxygen species (ROS). Hematopoietic stem cells (FDC-P1) were co-cultivated with plateau phase bone marrow primary stromal cell cultures from DBA/2 mice that were irradiated with 0.1-5 Gy of 120 keV/μm ^{4}He ions. FDC-P1 cell growth in the absence of IL3, induction of detectable IL3, and induction of malignant transformation of FDC-P1 cells were assessed by a colony growth assay. Growth data demonstrate that FDC-P1 cells grew rapidly and no longer required IL3 for growth indicating that they had been transformed by the exposure. Transformation of FDC-P1 cells was assessed using the morphology transformation assay. The results demonstrated that the irradiation of bone marrow stromal cells by alpha particle radiation causes an increase in the transformation of un-irradiated FDC-P1 cells. Some of the non-transformed FDC-P1 survivors were selected and expanded into culture to be tested for genetic instability.

Oliver Hobert of the department of Biochemistry and Molecular Biophysics of Columbia University is examining the radiation response of the nematode *C. elegans* (Exp. 144) using the Permanent Magnet Microbeam (PMM). The small worms are placed into microfluidic worm clamps developed at RARAF, which eliminates the need to anesthetize the worms and speeds up the irradiations, since the time in locating and targeting the worms is greatly reduced. The fixture is placed on the PMM end station and the worms are irradiated with 4.5 MeV protons. DNA damage in wild type *C.elegans* is assessed by the formation of Rad51 foci that are essential for homologous repair of radiation-induced DNA damage. The findings were validated by the use of a *C. elegans* strain mutant for Rad51 protein.

Rad9 has been implicated in a wide range of cellular processes (including the regulation of cell cycle checkpoints and DNA damage repair) that are thought to play roles in the development of tumors. Howard Lieberman continued investigations of the effects of Rad9 on radiation-induced changes in gene expression in human cells directly irradiated or as bystanders (Exp. 152). The human non-small cell long carcinoma cell line H1299 was used as the model system. Using shRNA against RAD9, the expression of RAD9 was knocked down in this cell line. Both parental and RAD9 knocked-

down cells were seeded onto double-ring "strip" dishes and irradiated with 1 Gy of ^{4}He ions using the Track Segment Facility. The outer ring has a 6 µm Mylar bottom through which the cells are irradiated by the ^{4}He ions while the inner dish has strips of 38 µm Mylar, which stop the ions. After irradiation, bystander response was measured by the micronucleus assay. They observed an increase in micronucleus count in the RAD9 knockdown cells as compared to the parental cells, which suggests RAD9 plays a role in radiation-induced bystander effect. Future studies will investigate the mechanism and the factors involved in this process.

Brian Ponnaiya of the CRR completed a study of the production of γH2AX foci by low-energy x-rays using the x-ray Microbeam Facility (Exp. 157). Cells were irradiated in media with 0.1 and 0.2 Gy of 4.5 keV x rays. The γH2AX foci were detected using anti human γH2AX monoclonal antibody, visualized using an Alexa Fluor 555 secondary antibody, and the nuclei were counterstained with DAPI. Fluorescent images were acquired and mean fluorescence intensities of a minimum of 150 individual cells were measured. The total nuclear fluorescence increased with dose and for 0.2 Gy was more than 3 times the intensity for controls. The variation in intensity between cells for both x-ray doses was significantly larger than for controls.

An experiment was initiated by Lubomir Smilenov and Erik Young of the CRR to determine if micro-RNAs (miRNAs) are a component of the bystander communication of radiation damage information (Exp. 159). A target population for irradiation is stained with Hoescht 33342 dye and then plated in co-culture at a ratio of 3:7 with unstained (bystander) cells containing green fluorescent protein (GFP) that is activated when a particular mRNA is present. The stained cells are irradiated with ^{4}He ions using the Microbeam Facility. Post irradiation, cells are sorted to separate the targeted cells with the Hoechst dye from the bystander cells, which are lysed and analyzed by PCR. This experiment required the development of the manual cell sorting system.

Ionizing radiation-induced reactive oxygen species (ROS) are thought to contribute to genomic instability and ultimately to cancer. Doug Spitz of the University of Iowa in collaboration with Manuela Buonanno began an investigation into the cellular oxidation of radiation-induced free radicals (Exp. 160). It was observed that following both nuclear and cytoplasmic irradiations, elevated levels of, presumably, superoxides were generated in the nuclei of mouse embryo fibroblasts irradiated with ^{4}He ions using the Microbeam Facility, as tested by MitoSOX (Figure 1) and DHE dyes. The results were validated by inhibiting nuclear oxidases with DPI. Since MitoSOX and DHE are not specific, in that the fluorescence could be due to intracellular or mitochondrial superoxides, and the emission spectra of the two fluorescent species are overlapping and difficult to separate by standard fluorescence microscopy, further

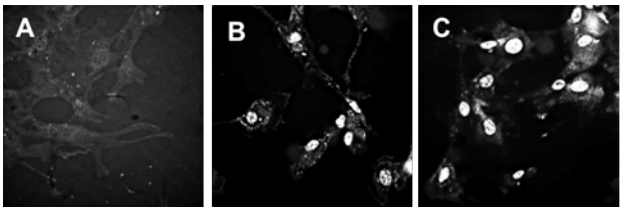

Figure 1. *MitoSOX fluorescence in control (A), nuclear irradiated (B) and cytoplasmic irradiated (C) MEFs 5 minutes post microbeam irradiation.*

irradiations will need to be performed. The two dyes will be separated by capillary electrophoresis and detected by laser induced fluorescence detection (CE-LIF).

Jan Vijg of the Albert Einstein College of Medicine, in colaboration with Brian Ponnaiya, has started an experiment to detect random, low-abundance mutations in mouse embryo fibroblasts after irradiation of the nucleus with 4He ions using the Microbeam Facility (Exp. 161). To enable the detection of these mutations, the whole genome of a representative number of single cells is sequenced. The approach combines single-cell-based whole genome amplification and high-throughput sequencing. Conditions have been optimized for the isolation of irradiated cells to provide material for successful whole genome amplification. Development has included writing new routines for the control of the microbeam stage to position individual cells at the point of the 50 µm diameter needle used to pick up the cells, developing protocols for the efficient re-positioning of the probe holder and determining the appropriate buffer in which the cells are collected. This has resulted in ~30% success rate as determined by the locus dropout test (Figure 2).

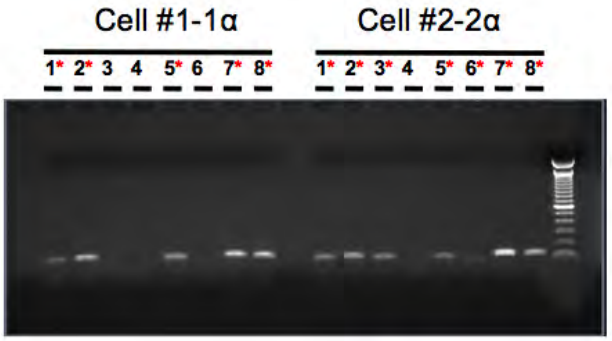

Figure 2. *Locus dropout test to determine whether the whole genome amplification is biased. Cell #1 was irradiated with 1 alpha particle and cell #2 with 2 particles (both randomly through the nucleus). 1-8 are the panel of PCR primer pairs. * indicates successful amplification.*

Lubomir Smilenov and Manuela Buonanno of the CRR are examining the role of connexin 43 (cx43) in the bystander effect *in vivo* by irradiating portions of the ears of hairless mice using the Microbeam Facility (Exp. 163). The mouse ear measures approximately 13 mm in both length and width with an average thickness of 250 µm. Mice were produced using the cx43 conditional knockout mouse model developed at RARAF. The transduction

vector was injected into a spot on one ear of the mouse, the area marked and later inspected to observe expression of GFP. A special fixture has been designed and constructed in the CRR machine shop to position anesthetized mice so that a region on one ear can be irradiated with the microbeam, the other ear serving as a control. The proton beam was defocused to a diameter of ~35 μm and scanned in a line a few mm long in order to irradiate a larger number of cells in the area of the transduction. After irradiation in the transfected area, the ears were sectioned transversely to the irradiated line and assayed for γH2AX and 53BP1 foci as a function of distance from the irradiation point.

A Rapid Automated Biodosimetry Tool (RABiT) is being developed at the CRR as a completely automated, ultra-high throughput biodosimetry workstation to screen tens or hundreds of thousands of individuals for radiation exposure to γ rays following a large-scale radiological event. The system uses the Cytokinesis Block Micronucleus assay (CBMN) and the γ-H2AX assay. Its utility is being extended to neutron irradiation by making use of the broad-spectrum neutron spectrum developed at RARAF (described below) that mimics the Hiroshima atomic bomb spectrum. Whole body irradiations of C57Bl/6 mice using this neutron spectrum have been initiated by Lubomir Smilenov (Exp. 164) and irradiations of human blood *ex vivo* by Helen Turner (Exp. 165), both of the CRR. The Hiroshima spectrum requires a combined beam of single, paired and triple protons and deuterons whose mix still is being developed. As an initial test, a beam of 5.0 MeV deuterons was incident on a thick beryllium target, producing neutrons with a known broad spectrum. Mice were given doses of 1 and 2 Gy of neutrons and 1 Gy of neutrons + 2 Gy of x rays and 2 Gy of neutrons + 4 Gy of x rays. T cells, B cells and cells with the common leukocyte marker CD45 were counted in blood samples taken from the mice 7 days after irradiation. There were significant reductions in all measurements, particularly after the highest doses, and future irradiations will use lower doses. The human blood was given doses of 0.5 Gy and 1 Gy of neutrons and combinations of these doses with 4 Gy x rays. Cell counts for the common leukocyte marker CD45 were determined at 2 and 24 hours after irradiation and high quality RNA (A260/230 >1.8) was isolated.

Andre Nussenweig of the NCI has begun a study of chromatin restructuring as a function of induced DNA double strand breaks (DSBs) using the microbeam (Exp. 166). The UV microspot is used to photoactivate a single spot in HeLa cells containing a photoactivatable version of GFP-tagged histone H2B (H2B-PAGFP). This spot will be targeted by the microbeam and irradiated with 1-10 ^{4}He ions. Cells will be fixed at 15, 30, 60 and 180 minutes post irradiation and assayed for γH2AX foci formation. In addition, live cell imaging will be used to follow the photoactivated spot as a function of time following microbeam irradiation with ^{4}He particles for up to 180 minutes. Corresponding photoactivated spots within the same cell (but not irradiated) at 1 and 2 μm from the irradiated spot will be monitored to assess alterations in undamaged chromatin as a function of distance from DSBs. Preliminary tests are ongoing to determine the minimum laser power required to activate a sufficient amount of GFP in as small an area as possible.

A study to investigate radiation-induced DNA damage in bystander cells in cells with inducible gap junction intercellular communication (Exp. 167) was initiated by Eduoard Azzam of the University of Medicine and Dentistry of New Jersey (UMDNJ) in collaboration with Manuela Buonanno. Ten percent of the nuclei of HeLa cells negative for cyclooxigenase2 (cox2) expression with chemically inducible connexin 26 (cx26) are irradiated with one ^{4}He ion. Compared to controls, both cx26 positive and negative cells exhibited a significant increase of cells with γH2AX foci; however, chemical induction of cx26 reduced the level of foci.

Roger Howell, also of the UMDNJ, in collaboration with Manuela Buonanno has started an investigation of bystander effects in an *in vivo*-like system as a function of the distance from irradiated cells (Exp. 168). Normal human fibroblasts (AG1522) mixed in a biogel (Matrigel) are loaded onto 3D carbon foam scaffolds (cytomatrices) 8.75 mm in diameter and 2 mm thick and irradiated with ^{4}He ions using the Track Segment Facility. The ions have a range of ~35 μm in the cytomatrix, so that only the first few cell layers are irradiated; the cells beyond the particle range are bystanders. *In situ* assays are performed to investigate DNA damage, cell death and micronucleus formation. The best results were obtained for radiation-induced 53BP1 foci formation. Cells with foci could be detected up to 60 μm away from the irradiated cell layer; no foci were observed 140 μm away.

Vincent LiCata of Louisiana State University is investigating whether proteins from radiation resistant organisms are radiation resistant in isolation (Exp. 169). This project will examine homologous DNA binding proteins from organisms that live under very different conditions, one being the extremely radiation-resistant bacterium *Deinococcus radiodurans*. Protein stability and function will be assayed at different radiation doses to determine whether the DNA polymerase (and eventually other isolated proteins) from *D. radiodurans* are better able to withstand radiation exposure than are homologous proteins from non-radiation resistant organisms. The project is focused primarily on so-called secondary radiation effects such as reactive oxygen species damage rather than direct hit effects, as the secondary effects are responsible for the majority of damage in biological systems. Protein in solution is formed into uniform thin layers by micropipetting the solution onto a standard Mylar track segment irradiation dish and placing a 22 x 22 mm^2 cover slip on it. The liquid spreads out by capillary action. In order to obtain sufficient material, multiple samples have been given doses of 5 to 20 kGy of

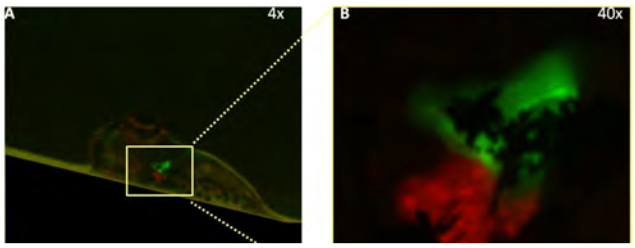

Figure 3*. Panel A: Outline of a zebrafish embryo 52 h post fertilization under the fluorescent microscope at RARAF (4x magnification). The zebrafish heart is delimited by the yellow rectangle. Panel B: The cells of the atrium are green fluorescent protein (GFP)-tagged and the cells of the ventriculum are red fluorescent protein (RFP)-tagged (40x magnification).*

4.0 MeV protons using the Track Segment Facility at dose rates in excess of 1 kGy/min.

In addition to charged particle irradiations, the ultraviolet (UV) microspot is being used as an irradiation modality by Kimara Targoff in the Division of Pediatric Medicine of Columbia University to observe the consequences of the ablation of single cells in the embryonic zebrafish heart (Exp. 162). Myocytes in the ventricles of the hearts of zebrafish embryos are transfected with red fluorescent protein (RFP) (Figure 3). Since the embryo is essentially transparent, this allows imaging of the cells in the ventricle for targeting by the UV microspot, which is then used to ablate the ventricle cells. An additional study is investigating the effect of local irradiation on heat shock protein (hsp) expression. Imaging of GFP-tagged hsp70 indicates that UV microspot irradiation of ventricular cells does not induce hsp expression either in the whole body or in the heart area, while x-ray irradiation induces a slight increase of hsp relative to controls.

Development of Facilities

Development continued on a number of extensions of our irradiation facilities and capabilities for imaging and irradiating biological specimens:

- Focused particle microbeams
- Focused x-ray microbeam
- Neutron microbeam
- Non-scattering particle detector
- Advanced imaging systems
- Targeting and manipulation of cells
- Small animal systems
- New neutron source

Focused particle microbeams

The electrostatically focused microbeam has continued to operate very reliably this past year, consistently producing a beam spot 1-2 µm in diameter using the standard 500 nm thick silicon nitride exit window. A window only 100 nm thick, which has a much smaller area and is more fragile, is used when a sub-micron beam spot is desired.

For quality control we perform a microbeam test run the evening before an irradiation so that the next morning, after the accelerator has warmed up, the charged particle beam is found immediately and has a minimal beam spot diameter. This provides an earlier and trouble-free start for irradiations and consequently a greater throughput.

Ceramic quadrupole triplet rods that were manufactured in our shop are being assembled into two new quadrupole triplets. They will be assembled in an alignment tube to replace the quadrupoles presently in use, which will become a spare set. The rods have been implanted with platinum ions at the Institute of High Current Electronics in Russia to increase the surface resistivity, which reduces ion charge build-up on the insulating sections between the electrodes, and have had a gold layer 1 µm thick plated on the electrode sections to make them conducting.

The permanent magnet microbeam (PMM) uses a compound quadrupole triplet lens system made from commercially available precision permanent magnets. Its design is similar to that of the electrostatic lens system for the sub-micron microbeam, the major difference being that it uses magnetic rather than electrostatic lenses. After tuning, it has consistently produced a ^{4}He beam spot 5 µm in diameter. The quadrupole magnet strengths used to focus the beam have been adjusted to produce a focused 4.4 MeV proton beam for development of the Flow and ShooT (FAST) microfluidics system, described below, and for irradiation of *C. elegans* nematodes.

Focused x-ray microbeam

We have developed a microbeam to provide characteristic K_{α} x rays generated by proton-induced x-ray emission (PIXE) from Ti (4.5 keV). A small x-ray source is produced by bombarding a Ti target with 1.8 MeV protons using a single electrostatic quadrupole quadruplet lens to focus the beam to ~50 x 120 µm on the target. Charged particle beams can generate nearly monochromatic x rays because, unlike electrons, they have a very low bremsstrahlung yield.

The x rays used are emitted at 90° to the proton beam direction. A zone plate 120 µm in diameter is used to focus the x-ray source to a beam spot 5 µm in diameter. The system is mounted on its own horizontal beam line on the 1st floor of RARAF and the x-ray beam is oriented vertically, so that the geometry of the microscope and stage is the same as for our charged particle microbeam systems.

Development of the facility has been completed and the first cell irradiations using the x-ray microbeam, an investigation of the production of γH2AX foci by low-energy x rays (Ponnaiya, Exp. 157), have been completed.

Neutron microbeam

Neutrons produced by the ^{7}Li(p,n)^{7}Be reaction are emitted only in a forward conical volume when the proton energy is just above the reaction threshold (1.881 MeV). The half-angle of this cone is dependent on the proton energy and increases with increasing energy. When

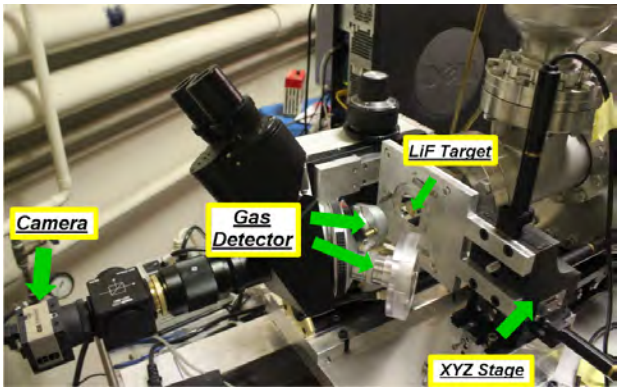

Figure 4. *Neutron Microbeam detection and imaging system.*

development is completed, a focused proton microbeam 5 μm in diameter will be incident on a 1 μm thick lithium fluoride target. The backing material will be 20-μm thick Au, selected for its high density and thermal conductivity, which will stop the incident proton beam. Using a 1.886 MeV proton beam, cells on a thin polypropylene substrate that is in contact with the target backing will be exposed to a beam of neutrons 20 μm in diameter having energies from 10-50 keV. This will be the first neutron microbeam in the world.

The facility has been constructed on a dedicated horizontal beamline using a single quadrupole quadruplet to focus the proton beam. The microbeam end station is shown in Figure 4. In order to measure the beam spot size, a thin Havar metal window is used in place of the gold target. The protons pass through this window and the beam spot size is determined in the same manner as for the PMM proton microbeam: a knife-edge scan using 10 μm thick tantalum strips in order to change the proton energy significantly. Unlike the other microbeams in which the charged particle or x-ray fluence is low, the proton beam current for the neutron microbeam is on the order of 1 nA ($6x10^9$ protons/s – too high to count) so an ionization chamber, instead of a solid state detector, is used to observe the change in the proton beam as it is scanned. The size of the neutron beam is measured using CR-39 track etchant plastic. Because the recoil protons generated by the neutrons do not make observable pits in the CR-39, the Cr-39 is coated with a thin layer of lithium carbonate heavily enriched in ^{6}Li. The neutrons interact with the ^{6}Li, producing energetic ^{4}He and ^{3}H recoils, which are easily observable as pits in the etched CR-39.

At present, the proton beam has been focused to a spot 20 x 25 μm with a beam current of 0.5 nA and measurements indicate a neutron microbeam ~80 μm in diameter. This is the first neutron microbeam in the world. A reduction in the diameter of the angle limiting aperture at the entrance to the quadruplet and further tuning of the quadruplet voltages will reduce the sizes of both the proton and neutron beam spots.

Non-scattering particle detector

The RARAF microbeam endstation presently delivers a precise number of particles to thin samples by counting the particles traversing them using a gas proportional counter placed immediately above the sample. Because the ^{4}He ions and protons used for irradiations have very short ranges (≤50 μm and <300 μm respectively), the medium over the cells must be removed to count the ions. To allow cell medium to remain in place during irradiations or to irradiate samples thicker than the range of the incident ions, a very thin particle detector is necessary between the beam exit window and the samples.

A silicon wafer 10±4 μm thick was cleaved into ~10 mm x 10 mm squares. Each square then was glued to standard glass microscope slides in which a 6 mm diameter hole had been drilled. A shadow masking procedure was used to deposit 100 nm thick gold and aluminum electrodes on one side of each silicon substrate to form a semiconductor detector. The opposite sides of the substrates were etched to different thicknesses using SF6 plasma in an inductively coupled plasma reactive ion etcher. Wires were attached to the electrodes using conductive epoxy. Calculations based on energy loss measurements using a proton beam produced thickness estimates of 13.5 μm, 11.5 μm, 11 μm, and 8.5 μm for the four detectors.

Current versus voltage (I-V) and capacitance versus voltage (C-V) tests that the devices constructed indeed behaved as diodes, as expected. Only the thinnest detector transmitted the standard ^{4}He ion beam with enough energy to be detected in the commercial semiconductor detector behind it. Measurements of the ^{4}He ion energy spectrum and count rate using the thinnest detector were consistent with measurements made using the commercial detector. Pulse height in the detector increased with distance from the gold electrode, however resolution decreased. On the other hand, for protons only the thickest detector (13.5 μm) produced pulses large enough to be above the electronic noise. Further studies will be performed to determine the effect of the detectors on the beam spot size.

Advanced imaging systems

We continue to develop new imaging techniques to obtain two- and three-dimensional images of cells without using stain. This is of great importance for the microbeam irradiation facilities in order to avoid damage to the cells and to image thick samples, especially small animals, for targeting and observation.

SIMI

Immersion-based Mirau interferometry (IMI) was developed at RARAF by constructing an objective to function as an immersion lens using standard interferometric techniques; however interferometry is very sensitive to vibrations, even as small as a fraction of a wavelength. Passive and active systems to reduce tiny vibrations on the microbeam end station were unsuccessful.

A new approach to overcome the vibration problem using Simultaneous Immersion Mirau Interferometry

(SIMI) was then developed at RARAF. In simultaneous Mirau interferometry polarized light is split into equal components in the x and y planes, one of which undergoes a phase shift of 90º by use of 1/8 wavelength (λ/8) waveplates. In the initial design a polarization beam displacer was used to send the x and y components to form interferograms on a single camera. Since the images are taken simultaneously, there is no effect from vibration. This approach simplifies alignment; however, the image resolution is limited because the separation distance of the beam-displacer defines the width of the field of view. A new beam splitter was obtained that splits the images into two separate cameras 90° to each other and uses the full resolution of each camera.

This system is not only vibration-independent but also much faster than Immersion Mirau because only one image is necessary instead of four images at different distances, requiring 3 vertical movements of the stage. SIMI is being incorporated into the sub-micron microbeam endstation as an imaging option for non-stained cell targeting and observation.

EMCCD

The Electron Multiplied Charge-Coupled Device (EMCCD) camera that was integrated into our charged-particle microbeam system has enabled us to improve our imaging practices, providing higher resolution images in shorter times and increasing sensitivity so that less fluorescent stain and UV are required. This resulted in higher throughput for microbeam irradiations.

To be able to observe short-term radiation responses (<1 min after exposure), we have developed techniques using the EMCCD camera's high sensitivity to image cells in a 'real time' movie acquisition. Initially transfer time was limited to a 1 second per frame. Modification this year of the computer routines for image transfer has resulted in reducing this time to 1/3 second, allowing more detailed observation of changes in cells.

UV Microspot

A multi-photon microscope was developed and integrated into the microscope of the Microbeam Facility several years ago to detect and observe the short-term molecular kinetics of radiation response in living cells to permit imaging in thick targets, such as tissue samples and *C. elegans*. Two photons delivered very closely together in space and time can act as a single photon with half the wavelength (and twice the energy). The longer wavelength of the incident light beam allows better penetration into the sample while still being able to excite fluorophors at the focal volume and less damage is produced in the portion of the sample not in the focal volume. By using the vertical motion of the microbeam stage, a series of images acquired at different depths in the sample can be assembled into a 3-D image.

Several users, both internal and external, have made use of this facility this year for 3-D imaging. This system is also being used as a laser "microspot" to induce UV damage in the cells in the ventricle of zebrafish embryos (Targoff, Exp. 162).

STED

The resolution of our imaging systems must be improved as we improve the focusing capabilities of our microbeam and irradiate ever-smaller targets. As reported last year, design has begun of a new microbeam system capable of focusing a charged particle beam to <100 nm. Our present imaging system is limited to a resolution of ~200 nm. Stimulated Emission Depletion (STED) has been selected as a super resolution system for the microbeam since it is compatible with our aim for rapid imaging and can be developed using our existing multiphoton microscope system as the excitation laser.

Stimulated emission happens at a specific lower energy state jump (longer wavelength) matching the STED illumination wavelength. Using a laser with longer wavelength (STED laser) than the fluorophor that is to be imaged to produce a ring of stimulated emission, it is possible to deplete the excited fluorophors around the edge of an excitation spot creating a sub-100 nm area where fluorescence is still possible. This concept is being extended to imaging in cell medium.

Initial tests of imaging live cell cultures using an immersion objective were made using the custom STED system developed by our Technical Consultant, Dr. Liao from the Mechanical Engineering Department at Columbia University. Although this system was not optimized for imaging through media, it was possible to locate single mitochondria with sub-100nm resolution in live cells. Our STED system will be based on the design used by Dr. Liao and requires the acquisition of a STED laser.

Targeting and manipulation of cells

Several of our staff now have been instructed on the use of the micro-milling machine purchased in 2011. They also have familiarized themselves with the software that programs the milling machine to produce a part that was designed using the Solid Works computer-aided design (CAD) program. This system has been used to manufacture the single cell dispenser and microfluidics chips for the FAST. It has eliminated the need to use Mechanical Engineering Department facilities at the Morningside campus of Columbia.

FAST

Development using the PMM is continuing on a Flow And ShooT (FAST) targeting system based on microfluidics to increase the throughput of the microbeam and to provide irradiation of non-adherent cells, such as lymphocytes, that do not plate on surfaces and therefore do not have stable positions.

Cells moving through a narrow channel are imaged by a high-speed camera (10s to 100s of frames/s) to track their trajectory. The Point and Shoot system is used to aim the particle beam to the projected position of the cell on the trajectory and the particle beam is enabled. The deflection coil currents are changed continuously to follow the path of the cell until the required number of

particles is delivered. The final system will be capable of tracking several cells at a time.

We manufacture polydimethylsiloxane (PDMS) microfluidic chips using soft lithography. The channel has a width of 200 µm and height of 20 µm, so that the cells, when targeted by the microbeam, flow in the immediate vicinity of the microbeam exit window. The bottom of the irradiation section of the microfluidic channel is 10 µm thick and the top is 20 µm thick, so particles can reach the cells and the detector above the channel. The flow rate is controlled by a syringe pump.

We previously have demonstrated targeting of cells moving ~100 µm/s and a throughput of 4,000-7,000 cells/hr, matching our dish-based microbeam. Recent implementation of high numerical aperture optics into the imaging system has allowed reduction of image acquisition time by a factor of 10 (from 20 to 1-2 msec) and work is ongoing to match this with a similar improvement in image processing speed, expected to result in an increase in cell irradiation throughput of a factor of net 3-10.

OET

Development continued on an Optoelectronic Tweezers (OET) system, a novel cellular manipulation technique for non-adherent cells (*e.g.* lymphocytes).

The OET consists of two parallel-plate indium tin oxide (ITO) electrodes separated by a 50 µm rubber gasket. The top electrode is transparent and is covered with a 1 µm thick layer of hydrogenated amorphous silicon (a-Si:H) that acts as a photoconductive layer (Figure 5). When light is focused on the surface of the silicon, the conductivity of the layer increases by several orders of magnitude. By patterning a dynamic light image on the electrode, a reconfigurable virtual electrode is created. When the two electrodes are biased with an AC voltage, a non-uniform AC field is created.

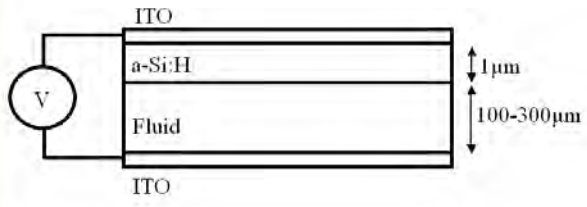

Figure 5. *Cross-section of an OET device.*

In the presence of a non-uniform electric field, a dielectric particle (*e.g.*, a cell) will feel a force caused by dielectric polarization (dielectrophoresis, DEP). The direction of the force is a function of the AC voltage frequency and the fluid conductivity. Below a certain frequency the cells are attracted by the force; at higher frequencies they are repelled. To better understand the system, the finite element software COMSOL Multiphysics Simulation has been used to simulate the electric field in the ET device.

Images can be created by any image production software and projected into the microscope using a standard LCD projector. This year the ability to manipulate fluorescently stained cells in solution and the transmission of the UV microspot, producing single strand DNA breakage in HT-1080 cells with GFP-tagged XRCC1, were demonstrated. Future work will include the fabrication of an OET device with a thin bottom substrate for charged particle microbeam irradiation.

Cell dispenser

Another cell manipulation device that is under development is a single cell dispenser. The dispenser consists of a microfluidic channel in which selected cells can be dispensed into a multi-well plate. In a system where cells normally travel across a T-intersection (Figure 6), a pressure pulse can eject a droplet containing a single cell as it passes the nozzle. The device is made from a polymethyl methacrylate (PMMA) slab with 100 µm x 50 µm channels directly milled using the micro-milling machine at RARAF.

Figure 6. *The cell dispenser showing the T-intersection.*

Presently this system is manual, very laborious and very inefficient, requiring the operator to observe cell fluorescence through a microscope and activate a switch to select the desired cells. Cell flow rate has to be kept low due to operator reaction time. An automated system is being developed to control the dispenser based on cell fluorescence or other selected criteria.

Probes

A non-invasive self-referencing biosensor/probe system developed by the Biocurrents Research Center, Marine Biology Laboratory (MBL) at Woods Hole for continuous measurement of ion fluxes from distinct regions around single cells has been installed on the microbeam end station. These probes can be used to selectively measure radical mediators, such as oxygen or nitric oxide. An offset hinge mounting system is used to position the tips of the probes in close proximity to selected cells.

To overcome the drift in the self-referencing amperometric microsensor response, the probe is cyclically moved through two fixed points in the extracellular ion gradient at a constant frequency. This

allows the drift measured at the reference point to be removed from the measurement at the point of interest.

A single-cell oxygen consumption measurement has been conducted with MBL oxygen probes immediately before and after microbeam exposure. A six-fold increase of oxygen flux induced by a single-cell irradiation was observed during a 15-second time period.

Small animal systems

C. elegans

C. elegans is a multi-cellular eukaryotic organism that is simple enough to be studied in great detail and is well-established as a research tool. It is small enough (~100 μm diameter, ~1 mm long) to be compatible with microbeam irradiation and a wide variety of mutants and transgenics are readily available, as is a large community of *C. elegans* researchers.

Initial irradiations required worms to be anesthetized and individually handled and located for irradiation manually - a slow and laborious process. In order to provide high-throughput irradiations, we developed, in collaboration with the Whitesides group at Harvard University, a microfluidic worm clamp for rapid immobilization of large numbers of live worms for morphological analysis and fluorescence imaging. The worm clamps have a 10 μm thick PDMS bottom to allow charged particle penetration. We have observed that the worms indeed remain immobilized without being anesthetized. The initial clamp design with four channels has been expanded to accommodate 16 worms with a possible further expansion to 64 worms.

Transgenic mouse model

One of the mechanisms for the propagation of bystander signals from irradiated to non-irradiated neighboring cells is cell-to-cell intercellular communication through gap junctions, with connexin 43 (cx43) being one of the major proteins involved; however studies on cx43's role in radiation-induced effects *in vivo* are limited by the fact that cx43 deficiency is embryonically lethal.

In order to produce a cx43 conditional knockout mouse model via lentiviral transduction, SKH-1E hairless mice are bred with the B6.129S7-Gja1tm1Dlg/J transgenic mice in which exon 2 of the cx43 gene is flanked by lox P sequences. This modification allows the complete knockout of the cx43 gene by transduction of cells with lentiviral vectors containing Cre recombinase. The viral vector also contains the green fluorescent protein (GFP) gene that renders only the cx43 knockout cells visible under a fluorescent microscope. The vector is injected into a spot on one ear of the mouse, the area marked and later inspected to observe the GFP. This transfection process has proven successful and is in use for microbeam irradiations (Smilenov, Exp. 163). Biological responses can be evaluated in irradiated versus non-irradiated regions of the ear and in cx43 knock-out mouse ears versus sham-irradiated ears.

New neutron source

Development has continued on a fast neutron source with a broad spectrum that will emulate that of the "Little Boy" atomic bomb at Hiroshima. A mixed beam of 5 MeV monatomic, diatomic and triatomic protons and deuterons incident on a thick beryllium target will produce neutrons from the $^{9}Be(d,n)^{10}B$ and $^{9}Be(p,n)^{9}B$ reactions. The diatomic and triatomic particles break up on contact with the target into individual ions with 2.5 MeV and 1.67 MeV energies, respectively, enhancing the lower-energy portion of the spectrum. In order to produce this mixed ion beam, a gas source with a specific ratio of hydrogen to deuterium will be placed in the terminal of our Singletron accelerator and a new, 0º beam line has been installed. Since this beam line does not involve deflecting the particle beam from the accelerator, there will be no separation of different ions and the full beam from the accelerator will be utilized.

A beryllium target with a high-capacity water cooling system has been designed and constructed. A gas detector containing a special gas mixture composed mainly of xenon and isobutylene will be used to determine the neutron spectra produced by 5 MeV, 2.5 MeV and 1.67 MeV protons and deuterons individually on beryllium in order to determine the ratio of hydrogen to deuterium required in the mixed beam that will produce a neutron spectrum. Our existing gas detector is capable of being filled only to three atmospheres of pressure, which would result in many high-energy recoil proton tracks being truncated at the wall of the chamber. A new chamber with a thicker wall capable of withstanding up to 10 atmospheres of pressure was ordered and has recently been received. This detector will make it significantly easier to deconvolute the proton recoil spectra to obtain the neutron spectra. As an additional method of neutron spectroscopy, an existing 2.5" D x 2.5" high liquid scintillation counter system has been refurbished.

The area in which the new 0º line has been constructed has much less shielding than the neutron cave that has traditionally been used for irradiations. A preliminary radiation survey was performed using a 5 MeV deuteron beam to identify areas that required additional shielding. Because of the high neutron dose rate that will be produced as well as the high energy of some of the neutrons, additional shielding has been added above the target position and in the maze entrance to the area. A support system was constructed to hold 6 layers of 4' x 4' x 1" thick polyethylene sheet over the target system to help shield the upper floors. A 5"-thick polyethylene door was added in the middle of the maze and 1" thick borated polyethylene was added to each side of the door to the area. An opening in the roof of the maze near the entrance has been covered with 8" of polyethylene. When the final neutron spectrum is available, the facility will be surveyed to determine if all areas are adequately shielded.

Preliminary irradiations of mice and human blood have been performed using 5.0 MeV deuterons on beryllium. The neutron spectra from this Be(d,n) reaction

have been measured at various angles by a group at Ohio State University. The Be target system was mounted on the end of the beam line in the neutron cave so that the only incident particles would be single 5.0 MeV deuterons. Mice were mounted in special tubes manufactured in our Design and Instrument Shop. The existing mouse rotator was positioned so that the centers of the mice were at the same position that will be used when the Hiroshima neutron spectrum is available. Neutron and gamma-ray dosimetry were performed with an ionization chamber and a compensated Geiger-Müller counter. Neutron irradiations of human blood were also performed. The end caps for the irradiation tubes made for the mice were modified so that blood collection tubes could be placed in them so that the blood was in the same position and could be irradiated in exactly the same manner as the mice.

Singletron Utilization and Operation

Table II summarizes accelerator usage for the past year. The Singletron normally is started between 8 and 9 am and the nominal accelerator availability is one 8-hour shift per weekday (~248 shifts per year), however the accelerator is frequently run well into the evening, often on weekends, and occasionally 24 hours a day for experiments or development. Total use for experiments and development this year was 99% of the regularly scheduled time.

Accelerator use for radiobiology and associated dosimetry was more than double that for last year and about 40% higher than the average for the last 5 years. About 80% of the use for all experiments was for charged particle microbeam irradiations (including the permanent magnet microbeam facility), 10% for track segment irradiations, 7% for x-ray microbeam irradiations and 3% for neutron irradiations. Approximately 1/4 of the experiment time was for experiments proposed by external users, and 3/4 was for internal users.

Table II.
Accelerator Use, January - December 2011
Usage of Normally Scheduled Shifts

Radiobiology and associated dosimetry	**47%**
Radiological physics and chemistry	**0%**
On-line facility development and testing	**44%**
Microbeam Training Course	**2%**
Safety system	**2%**
Accelerator-related repairs/maintenance	**0%**
Other repairs and maintenance	**2%**
Off-line facility development	**40%**

On-line facility development and testing was about 44% the available time, primarily for development and testing of the Flow and Shoot (FAST) system, the neutron microbeam, the self-referencing probes (SERP) and the Hiroshima neutron spectrum system. This was about average for recent years but almost 4 times as much as last year.

The accelerator was not opened for maintenance or repair this year and no accelerator-related repairs were required. This is the first time since RARAF was moved to Nevis Laboratories in 1982 that no accelerator repairs were made.

Training

We continue to participate in the Research Experiences for Undergraduates (REU) project in collaboration with the Columbia University Physics Department as we have since 2004. This is a very selective program that attracts talented participants. For 10 weeks during the summer students attend lectures by members of different research groups at Nevis Laboratories, work on research projects, and present oral reports on their progress at the end of the program. Among other activities, the students receive a seminar about RARAF and take a tour.

This year Brendan Burgdorf from Bucknell University participated in the program and worked with Gerhard Randers-Pehrson measuring fluctuations in the stray magnetic fields in the vicinity of the electrostatically focused microbeam beam line.

Microbeam Training Course

The second annual RARAF microbeam training course “Single-Cell Microbeams: Theory and Practice” was given March 19-21, 2012. The course was scheduled to allow integration with the 10th International Microbeam Workshop, which was held at Columbia March 15-17, 2012 (see Dissemination section). Several of the students and one guest lecturer, Dr. Hideki Matsumoto from the University of Fukui, Fukui, Japan, attended the Workshop as well. The course was extended from 6 participants to 8 participants this year, which is probably the largest number we can reasonably handle.

Dr. Marcelo Vazquez of Loma Linda University Medical Center again served as the Director. Dr. Vazquez has had significant experience with such courses from his prior employment at the NASA Space Radiation Laboratory (NSRL) at Brookhaven National Laboratory (BNL). He helped establish the first NASA Space Radiation Summer School and assisted in running the course for three years. He is familiar with the requirements of educating students on the utilization of specialized irradiation facilities.

Publicity:

- E-mail notifications using the contact lists for the previous course and the 2012 Microbeam Workshop.

- Announcements on the RARAF web site, and the EURADOS web site.

Applicants and Students:

- We received 22 applications. The prospective students again covered a wide range of educational levels, were from the U.S, Europe, Australia and Asia and were about evenly split in gender and field.
- The eight applicants selected for the course are listed in Table III and shown in Figure 7.
- Sekaran Sureka, an Assistant Professor from Bharathair University, India, participated as an observer.
- Jihua Nie, a Lecturer, and Jie Zhang, a Ph.D. student, both from Soochow University, Suzhou, China, audited the course, attending the lectures and receiving the course materials.

Day 1:

- Followed essentially the same format as the first course, with the inclusion of a guest lecture by Dr. Matsumoto.
- This year the RARAF tour was enhanced by a series of poster stations demonstrating new beam developments (X-ray and neutron microbeams, UV-microspot) and their use for biological studies.
- The day ended with a new session on the planning and experimental design of microbeam irradiations.

Day 2:

- Followed the format of the first year with demonstrations, hands-on activities, and intense debriefings (Figure 8).
- In addition, the students were tasked with designing an experiment based on their own scientific interest using knowledge obtained during the course to create a RARAF beam time request proposal.

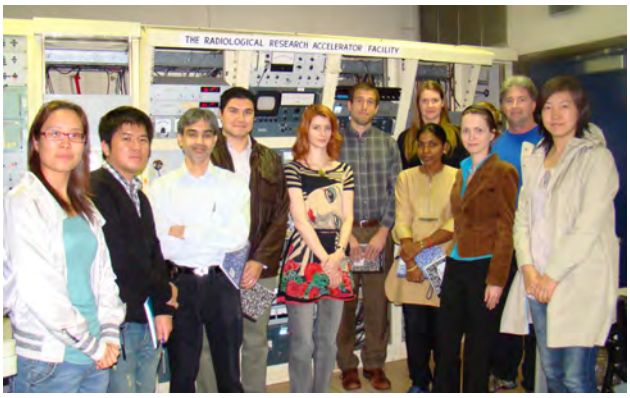

Figure 7. *The students for the second RARAF Microbeam Training Course, at the Singletron accelerator console.*

Day 3:

- Followed the format of the first year with lectures and group discussions.
- The lectures were followed by an intense discussion on user/facility interfacing.
- The students presented their individual or team beam-time proposals for review by the instructors.

Feedback and Outcome:

- The students' surveys indicated a high degree of satisfaction in all areas of the syllabus and laboratory activities.
- Suggested improvements included increasing the level of hands-on activities and extending the overall duration of the course up to five days in order to integrate more "real time" experiments and reduce the cramming of lectures and lab activities. These suggestions will be considered in the design of the next training course to be given in 2013.
- Adobe Acrobat versions of presentations and videos of lectures from this course were added to the RARAF web site and are discussed in the Virtual Training Course part of the Dissemination section.

Table III. Students for the second RARAF Microbeam Training Course.

Name	Position	Affiliation
Narongchai Autsavapromporn*	Postdoctoral Researcher	National Institute of Radiological Sciences (NIRS), Japan
Abdelrazek Abdelrazzak*	Postdoctoral Researcher	The New Jersey Medical School Cancer Center
Matthew Estes	Postdoctoral Researcher	The University of Arizona
Anne-Catherine Heuskin*	Ph. D. Student	University of Namur, Belgium
Sangeet Honey	Assistant Professor	SUNY Stony Brook
Bonnie Howe*	Biomedical Engineer	Australian Nuclear Science and Technology Organization
Evgenia Remeeva	Visiting Research Fellow	Warren Grant Magnuson Clinical Center, NIH
Robert Robinson*	Master's Intern	Pacific Northwest National Laboratory

**Attended Microbeam Workshop*

Figure 8. *Microbeam Training Course students engaging in hands-on training.*

- Movie clips from a lecture and a hands-on instruction session can be viewed in the Appendix.
- A paper on the design of and our experience with the training course has been submitted for publication.

Dissemination

Web site

A new RARAF website design has been created that provides clear and effective presentation and improves access to content. The RARAF website (home page shown in Figure 9) features a more modern look, intended to attract future microbeam users with updated content to reflect the current state of research at RARAF. Functional menus (including a home page rotating-picture menu) were designed to make navigation through the content easy and interesting, with a hierarchical structure from general information, suitable for a general or non-science audience, down to more detailed technical content. Primary sections in the new website are:

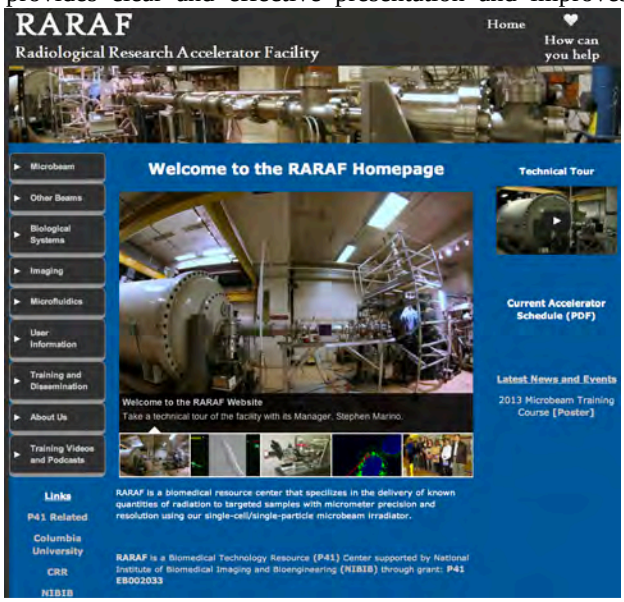

Figure 9. *Newly re-designed RARAF home page.*

- **Microbeam**, which contains general information on microbeams, as well as detailed technical information on our various microbeams.
- **Biological Systems**, which includes general information about various *in-vitro* and *in-vivo* endpoints that we use, again with the option to dig deeper for more technical information.
- **Imaging**, which has subsections for online imaging, offline imaging, and multiphoton imaging.
- **Microfluidics**, which contains a general introduction, as well as sections on optoelectronic tweezers, cell sorting, cell dispensing, and their applications to flow and shoot microbeams.
- **Other RARAF Beams,** contains information about our "broad beam" charged particle irradiation facilities, our fast neutron, and our slow neutron facilities.
- **User Information**, which contains information for current and future users, such as Collaboration-based and Service-based application forms, current scheduling forms, and current accelerator schedules.
- **Training and Dissemination:** In the Training section are multiple training videos that we have produced, which constitute our online microbeam training course, together with synched PowerPoint slides and downloadable PDFs. In the Dissemination sections are details of the international microbeam workshops that we have organized, our "face-to-face" microbeam training course, complete publications lists, lists of all talks given by RARAF staff and collaborators, as well as past RARAF annual reports.
- In **About Us**, there is a section on the history of RARAF, contacts and directions, as well as links to other related P41 facilities (*e.g.*, The Developmental Resource for Biophysical Imaging Opto-Electronics, Cornell University).

Virtual training course

We have developed an on-line virtual microbeam training course, based on the three-day microbeam training courses "*Single-Cell Microbeams: Theory and Practice*" held at RARAF in 2011 and in 2012. This training course, described in more detail below, was designed to give interested physicists and biologists a thorough and hands-on introduction to microbeam technology.

The goal of the online course, as for the face-to-face course, is to facilitate a better understanding of how